Investigation of Cobalt Alloy L605 as an Effective Oxygen Evolution Reaction Catalyst

Craig Moore and Dev Chidambaram*

University of Nevada, Reno, 1664 N Virginia St. MS 0388 Reno, NV 89557 USA

*Corresponding author, dcc@unr.edu

Abstract

Identifying stable materials with facile kinetics for the oxygen evolution reaction is an important step in decreasing the cost associated with the production of hydrogen from water. In this study, a previously unexplored alloy, alloy L605, was evaluated for its ability to catalyze the oxygen evolution reaction and results were compared to Nickel 200 and pure cobalt. Alloy L605 required an overpotential of 420 mV to achieve a current density of 10 mA/cm^2. The overpotential was found to lower required for Nickel 200 and cobalt. Also, the surface composition of the alloy was analyzed to obtain insight into the catalytic surface.

Keywords

OER; XPS, Alloy 25, Co alloy

Introduction

To prevent significant environmental change in the future, investment into energy sources that do not produce greenhouse gases is important [1]. One carbon-free energy source that can be produced and stored is hydrogen gas. Stored hydrogen gas can produce usable energy in a fuel cell through a redox reaction involving the reduction of oxygen and the oxidation of hydrogen gas to produce water [2]. One method to produce hydrogen gas is through the catalytic breakdown of water, which results in the formation of hydrogen and oxygen gases at the cathode and anode, respectively. The production of hydrogen is hindered by the sluggish kinetics associated with the oxygen evolution reaction (OER), which increases the overall energy requirement for the production of hydrogen gas [3].

Considerable efforts are being made to identify materials that increase the kinetics for the OER in various aqueous conditions, and reviews on current research directions can be found elsewhere [4-6]. The kinetics of the OER can be increased by identifying anode compositions that better catalyze the reaction or by developing materials with increased electroactive surface areas. One common method to create such electrocatalysts is by depositing precursor compounds onto conductive substrates, allowing the deposited material to be analyzed without synthesis of a monolithic electrode [4-6]. There are two risks to this approach. (i) potential anodic dissolution will result in the expulsion of the surface catalysts and (ii) oxygen evolution can lead to bubbling and removal of the active material, resulting in decreased performance over time [5]. A route to explore materials that avoids this risk is to analyze the catalytic ability of the oxidized surface that forms on alloys. Anodic polarization in electroactive alloys will result in the formation of a surface layer, which will create an interface where catalytic activity occurs. It has been predicted that changes in bond length due to alloying will alter the catalytic properties of a material [7], thus, investigation of unique alloy compositions may result in the discovery of novel, efficient catalysts. In this study, the oxidized layer formed on alloy L605 was evaluated for its ability to act as a catalyst for the oxygen evolution reaction. It should be noted that alloy L605 is commercially available. Commercial, bulk alloys enjoy the advantage of being available at industrially-relevant volumes, ability to be prepared into any required shape/form and have the robustness of a thick sheet metal when compared to surface adsorbed catalysts. Nickel 200 and pure cobalt were also analyzed to act as a benchmark for the results found. Additionally, X-ray

photoelectron spectra for the Co $2p_{3/2}$ and the O 1s features was recorded to provide insight into the interface composition of Alloy L605.

Materials and Methods

2.1 Materials

Nickel 200 (McMaster-Carr), 99.95% pure cobalt (Thermo Fisher-Scientific) and alloy L605 (VDM metals) were obtained and mechanically polished with sand paper. The polished samples were rinsed with deionized water and ultrasonicated in isopropanol for 5 minutes. The vendor supplied composition range for alloy L605 is shown in Table 1.

2.2 Electrochemical Testing

All samples were tested in a three-electrode configuration with a platinum/niobium mesh counter electrode, a Hg/HgO reference electrode and the sample of interest acting as the working electrode. The working electrodes had a geometrical area of 1 cm^2 for each experiment. Experiments were conducted in duplicates to ensure repeatability. The electrolyte for all measurements was comprised of a 1M NaOH solution prepared from analytical grade NaOH pellets (VWR Life Science) and deionized water. Electrochemical measurements were performed and recorded using a Gamry Reference 3000 potentiostat. All recorded potentials were shifted from the reference Hg/HgO scale to the reversible hydrogen electrode (RHE) scale through the equation $E_{RHE} = E_{Hg/HgO} + .098\ V + .059 \times pH$. Linear sweep polarizations were performed from 1.2V to 3.2V vs RHE at a scan rate of 5 mV s^{-1}. Reported potential values are iR compensated.

2.3 Characterization

X-ray photoelectron spectroscopy (XPS) spectra from alloy L605 prior to and after electrochemical studies were collected using a ThermoFisher Scientific Nexsa G2 Surface Analysis System with a monochromatic Al X-ray source. A 400 µm spot sized was selected and spectra were charge corrected to the C 1s peak of adventitious

carbon at 248.6 eV. Before spectra were obtained, the surface was cleaned with a 1000 eV argon ion source for 10 seconds.

Results and Discussion

The potentiodynamic polarization scans are shown in Figure 1. All three materials tested exhibited an initial decrease in current density with increasing potential. This behavior can be attributed to the development of a corrosion layer that limits the kinetics for the corrosion reaction. Above a potential of 1.49V vs RHE, the current density began to increase and logarithmic current density was found to be linearly proportional to potential. Linear Tafel region existed between potentials of 1.54V to 1.63V vs RHE as indicated in Figure 1. Tafel slopes were found to be 74, 58 and 66 mV/decade for cobalt, alloy L605, and nickel 200, respectively. The low Tafel slope for alloy L605 indicates superior oxygen evolution kinetics. Deviation from expected Tafel behavior was encountered beyond the specified region due to the formation of oxygen bubbles on the electrode surface which imposed mass transport limited conditions. At high overpotentials, the noise present in the data is attributed to the release and reformation of oxygen bubbles from the electrode surface [8].

The linear sweep voltammograms presented in Figure 2 indicate that alloy L605 required the lowest overpotential of 420 mV to achieve the benchmark current density of 10 mA cm^{-2} as shown by the horizontal dashed line. Nickel 200 and cobalt required overpotentials of 432 mV and 446 mV, respectively, to achieve the same current density. This indicates that alloy L605 has superior catalytic performance for the oxygen evolution reaction compared to nickel 200 and pure cobalt.

Figure 3 contains the XPS spectra for the Co $2p_{3/2}$ and the O 1s peaks for alloy L605 prior to and after electrochemical studies. The lowest binding energy peak is indicative of metallic cobalt and the higher energy peaks correspond to a primary oxidized peak and a satellite peak [9]. The cobalt spectra shown in Figure 3a clearly shows a strong metal signal on the sample prior to electrochemical studies (control) which is not seen on sample after electrochemical studies. The peak profile from the sample analyzed after electrochemical studies corresponds most closely to the $CoOH_2$ profile published by Biesinger *et al.*[9], suggesting that metallic cobalt was oxidized during testing and that the hydroxide concentration on the surface increased. The O 1s spectra in Figure

3b reveals an increase in intensity for the cobalt hydroxide peak at 530.87 eV and a decrease in intensity for the lattice oxide peak at 529.59 eV when comparing the samples analyzed after and prior to electrochemical testing [9]. This result further supports the formation of cobalt hydroxide during electrochemical testing.

Of the materials tested, alloy L605 exhibits the best catalytic activity for the oxygen evolution reaction. The presence of chromium in alloy L605 is likely responsible for the increased kinetics experienced, as it has been shown that cobalt alloyed with chromium results in more facile kinetics [10]. Despite the increased kinetics experienced on alloy L605 for the reaction, other transition metal catalysts have previously shown even better kinetics for the reaction. A Ni-Co-Fe catalyst previously prepared and tested in our laboratory under similar conditions required an overpotential of 300 mV to achieve a current density of 10 mA cm^{-2} [11]. Similarly, many other transition metal-based catalysts require overpotentials less than 400 mV to achieve the benchmark current density in alkaline conditions. However, differences in electroactive surface areas may exaggerate the discrepancy in performance [4-6].

Conclusion

Alloy L605 exhibited greater catalytic capability for the oxygen evolution reaction relative to nickel 200 and pure cobalt. The alloy had a Tafel slope of 58 mV/decade and required an overpotential of 420 mV to achieve a current density of 10 mA cm^{-2}. Although the alloy had less facile kinetics than some previously explored transition metal-based catalysts, its commercial availability, shape-forming flexibility, and robustness of a sheet metal makes it a competitive option for the electrolysis of water. Decreasing the financial barrier to hydrogen gas production through water electrolysis will improve the probability of transition to a hydrogen-economy.

Declaration on Interests

The authors declare that they have no known competing financial interests or personal relationships that could have appeared to influence the work reported in this paper.

Acknowledgements

The authors thank Jeremy Moon and Jerry Howard for proof reading and assistance. The purchase of the X-ray photoelectron spectrometer, housed in the Materials and Electrochemical Research Laboratory, was supported by the National Science Foundation through NSF MRI award 2117820. This research was funded in part by the US Nuclear Regulatory Commission (USNRC) under contract 31310018M0032. Ms. Nancy Hebron-Isreal serves as the program manager for the NRC award.

References

[1] M.S. Dresselhaus, I.L. Thomas, Nature 414 (2001) 332-337. https://doi.org/10.1038/35104599

[2] R.-A. Felseghi, E. Carcadea, M.S. Raboaca, C.N. Trufin, C. Filote, Energies 12 (2019) 4593. https://doi.org/10.3390/en12234593

[3] I. Katsounaros, S. Cherevko, A.R. Zeradjanin, K.J.J. Mayrhofer, Angew. Chem. Int. Ed. 53 (2014) 102-121. https://doi.org/https://doi.org/10.1002/anie.201306588

[4] H. Zhong, C. Campos-Roldán, Y. Zhao, S. Zhang, Y. Feng, N. Alonso-Vante, Catalysts 8 (2018) 559. https://doi.org/10.3390/catal8110559

[5] M.-I. Jamesh, X. Sun, Journal of Power Sources 400 (2018) 31-68. https://doi.org/https://doi.org/10.1016/j.jpowsour.2018.07.125

[6] G.A. Gebreslase, M.V. Martínez-Huerta, M.J. Lázaro, J. Energy Chem. 67 (2022) 101-137. https://doi.org/https://doi.org/10.1016/j.jechem.2021.10.009

[7] S. Saha, A.K. Ganguli, ChemistrySelect 2 (2017) 1630-1636. https://doi.org/10.1002/slct.201601243

[8] S.H. Ahn, I. Choi, H.-Y. Park, S.J. Hwang, S.J. Yoo, E. Cho, H.-J. Kim, D. Henkensmeier, S.W. Nam, S.-K. Kim, J.H. Jang, ChemComm. 49 (2013) 9323. https://doi.org/10.1039/c3cc44891f

[9] M.C. Biesinger, B.P. Payne, A.P. Grosvenor, L.W.M. Lau, A.R. Gerson, R.S.C. Smart, Appl. Surf. Sci. 257 (2011) 2717-2730. https://doi.org/https://doi.org/10.1016/j.apsusc.2010.10.051

[10] C.-C. Lin, C.C.L. Mccrory, ACS Catal. 7 (2017) 443-451. https://doi.org/10.1021/acscatal.6b02170

[11] M.L. Lindstrom, R. Gakhar, K. Raja, D. Chidambaram, J. Electrochem. Soc. 167 (2020) 046507. https://doi.org/10.1149/1945-7111/ab6b08

Table 1: Certified wt % composition for alloy L605

	Ni	Cr	Fe	C	Mn	Si	Co	W	P	S
Alloy L605	10.61	20.64	2.6	.075	1.69	.001	49.09	14.79	.007	.001

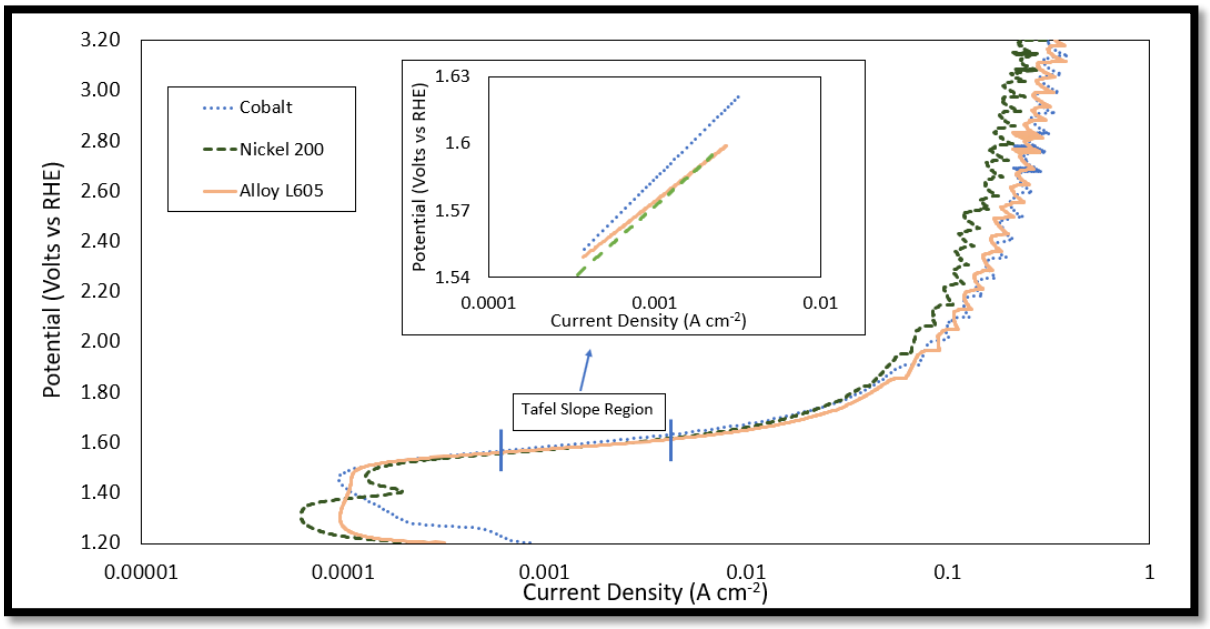

Figure 1: Tafel plot for the linear sweep polarizations performed on Nickel 200, alloy L605 and pure cobalt.

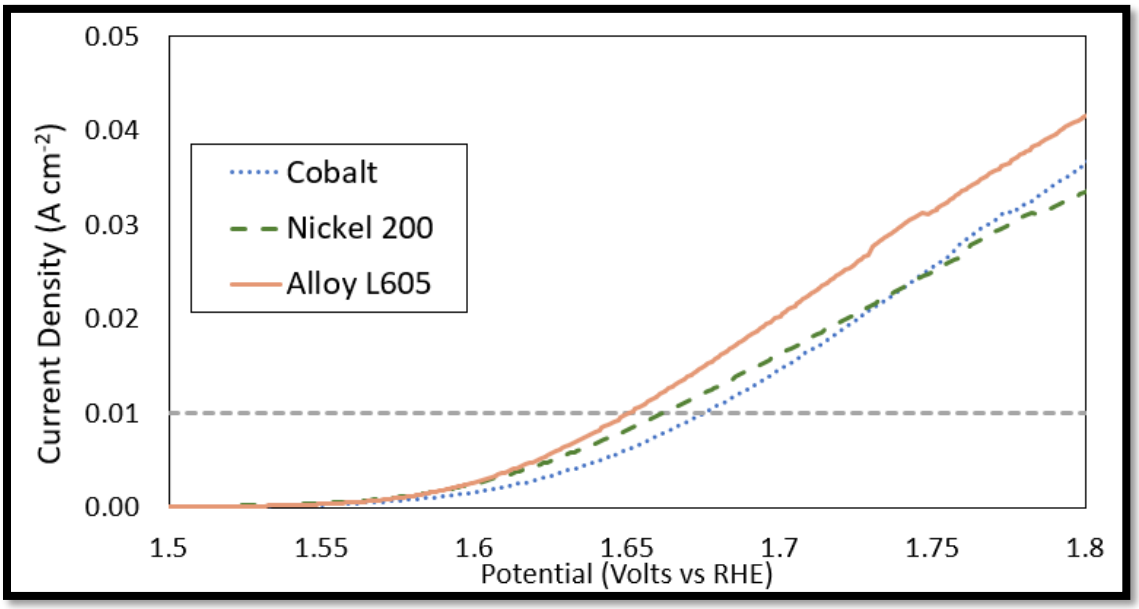

Figure 2: Linear sweep voltammograms for nickel 200, alloy L605 and cobalt.

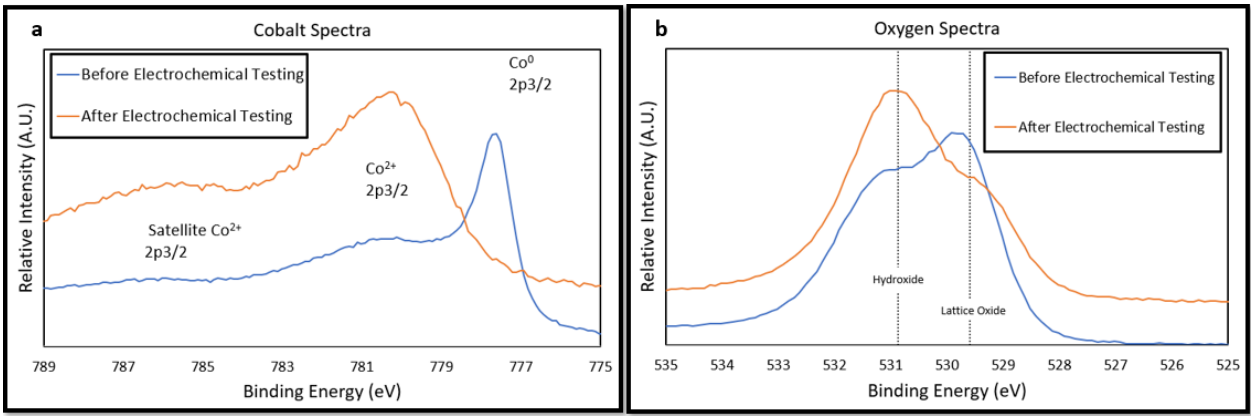

Figure 3: XPS spectra for Alloy L605 prior to and after electrochemical testing of Co 2p3/2 (a), and O 1s curves (b).